High transmission nanoscale bowtie-shaped aperture probe for near-field optical imaging

Liang Wang and Xianfan Xu[a)]
School of Mechanical Engineering, Purdue University, West Lafayette, Indiana 47907

(Received 12 March 2007; accepted 5 June 2007; published online 25 June 2007)

A near-field scanning optical microscope probe integrated with nanoscale bowtie aperture for enhanced optical transmission is demonstrated. The bowtie-shape aperture allows a propagating mode in the bowtie gap region, which enables simultaneous nanoscale optical resolution and enhanced optical transmission. The optical characteristics of the bowtie aperture are demonstrated by measuring the optical near fields produced by the aperture. It is shown that bowtie aperture probes have one order of magnitude increase in transmission over probes with a regular shape aperture of the same resolution. The imaging results using bowtie aperture are in agreement with those obtained from numerical calculations. © *2007 American Institute of Physics*. [DOI: 10.1063/1.2752542]

Since the demonstrations of the near-field scanning optical microscope (NSOM) in 1984,[1,2] NSOM systems with subwavelength resolution have become an important tool in many application fields, including single molecule detection,[3] nanofabrication,[4] and high density data storage.[5] The simplest way for obtaining nanoscale optical resolution is to employ a nanoscale aperture in a metal screen.[6] Many NSOMs use such a nanoscale aperture, called aperture-NSOM, to achieve subwavelength resolution.[1,2] For aperture-NSOMs, the size of the aperture at the apex of the probe determines the ultimate optical resolution. Nowadays, tapered optical fibers and microfabricated cantilever aperture probes are commercially available, benefiting from the rapid development of various fabrication techniques. The most widely used aperture probe consists of a tapered optical fiber obtained by heating and subsequent pulling to create an aperture smaller than 100 nm.[1,2] Another method for manufacturing aperture NSOM probes is by wet chemical etching to produce a taper with a sharp end point.[7,8] However, commercial NSOM probes suffer from poor transmission efficiency due to the wavelength cutoff effect, therefore light cannot be efficiently coupled through.[9,10]

To improve the optical transmission efficiency through nanoscale apertures, a special type of nanoaperture in a bowtie shape as well as its opposed part the bowtie antenna has been investigated recently.[11–15] As shown in the top of the left column in Fig. 1, a bowtie aperture has two open arms and a gap. Numerical[11,12] and experimental studies[16,17] have demonstrated that the bowtie aperture allows propagating waveguide mode in the gap region under properly polarized irradiation, which enables bowtie nanoapertures to simultaneously achieve nanoscale light concentration and enhanced optical transmission. It is also known that surface plasmon can enhance field transmission in noble metals. The difference of using the bowtie aperture is that it provides a broad band (from IR to UV) field localization and enhancement and does not need to use noble metal which can be soft (gold) or unstable in air (silver). There is also plasmonic effect in a bowtie aperture as studied in our earlier work,[11] which found that the plasmonic effect does not always localize the field since the plasmon is a surface wave which propagates along the surface and spreads the field.

As a high precision fabrication technique, focused ion beam (FIB) milling has been used for fabricating subwavelength aperture at a fiber tip and cantilever tip.[18,19] Here we investigate fabricating bowtie aperture on NSOM probe to utilize its superior optical characteristics. The transmission enhancement of bowtie apertures is demonstrated by comparing with comparable square apertures by far-field measurements. We then examine NSOM probes with nanoscale bowtie apertures fabricated at the probe apex by FIB machining. The capability of bowtie aperture probes for optical imaging is demonstrated by comparing with regular aperture probes using a homebuilt transmission-collection NSOM system. The experimental results are also compared with numerical simulations.

The bowtie apertures were fabricated using FIB milling. A 150-nm-thick aluminum film was deposited on a quartz

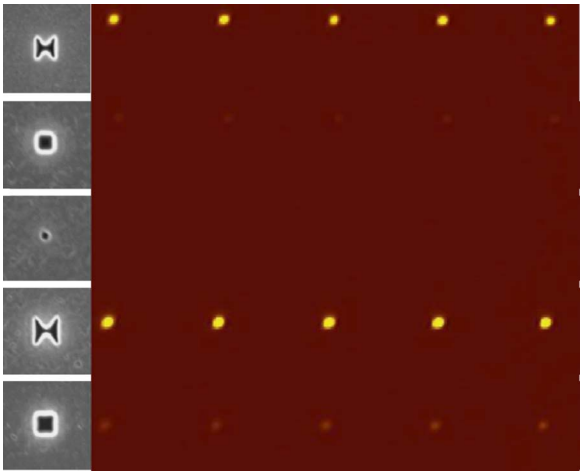

FIG. 1. (Color online) Left: scanning electron microscopy images of fabricated bowtie and comparable square apertures. From top to bottom: bowtie aperture with outline dimension of 160 nm, 105×105 nm^2 square aperture, 33×33 nm^2 square aperture, bowtie aperture with outline dimension of 180 nm, and 130×130 nm^2 square aperture. Right: far-field transmission measurement results of bowtie apertures and square apertures. The five images in each row are produced by five apertures of the same geometry to show the consistency of the measurements.

[a)]Author to whom correspondence should be addressed; electronic mail: xxu@ecn.purdue.edu

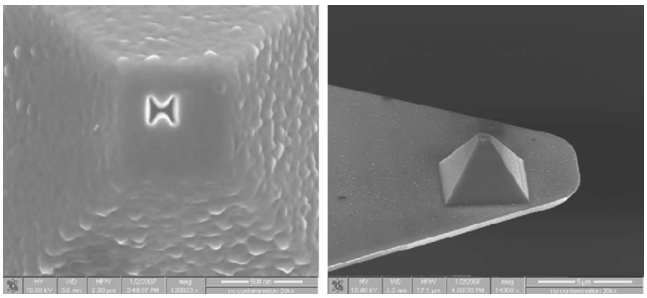

FIG. 2. Front and side views of a bowtie aperture probe. The bowtie aperture has a 180 nm outline dimension and a 33 nm gap.

wafer by e-beam deposition. Bowtie apertures with outline dimensions of 160 and 180 nm and a gap of 33 nm were fabricated. For the purpose of comparison, square apertures with dimensions of 105×105 nm^2 and 130×130 nm^2, having the same opening area as the two bowtie apertures, and a 33×33 nm^2 square aperture having the same area as the gap of the bowtie aperture were fabricated (left column of Fig. 1). Transmission of the apertures was measured using a 458 nm argon ion laser. The transmitted laser light through a single aperture in the sample is collected by a 50× objective lens and directed onto a photomultiplier tube (PMT). The sample was raster scanned and recorded by the PMT signal readout. The power throughput of each aperture can therefore be compared by the photon counts. The two bowtie apertures with outline dimensions of 160 and 180 nm had 100×10^3 and 160×10^3/s photon counts, respectively. On the other hand, there were only 5×10^3 and 15×10^3/s photon counts obtained from the two comparable square apertures. This indicates more than one order of magnitude higher transmission from bowtie apertures when compared to the square apertures with the same opening areas. The small 33×33 nm^2 square apertures did not transmit enough light to be detected by the PMT.

We then investigated using bowtie aperture on NSOM probes and compared them with regular aperture probes. The probe fabrication procedure is as follows. We started with standard silicon nitride cantilevered atomic force microscopy (AFM) probes, which had a pyramidal-shaped tip near the end of cantilever. On the tip of the probe, a platform was created by FIB side slicing. Then an aluminum film of about 100 nm thick was deposited to cover the entire tip side of the cantilever, including the platform. FIB drilling was then used to make bowtie apertures and regular square apertures through the aluminum film. The bowtie aperture fabricated on the NSOM probe has a 180 nm outline dimension with a 33 nm gap. Figure 2 shows the front and side views of a fabricated bowtie aperture probe.

The bowtie aperture probes were investigated using a homebuilt transmission-collection NSOM system. The sample was illuminated by an argon ion laser at a wavelength of 458 nm. The transmitted light through the apertures on the sample was collected by the NSOM probe and directed onto a PMT. A 75 μm pinhole was placed in the image plane of the objective lens to block the ambient light. Standard AFM feedback scheme based on light deflection was used to control the probe position. NSOM images were obtained by raster scanning the sample using a high precision piezoscanner and recording the optical signal from the PMT by photon counting.

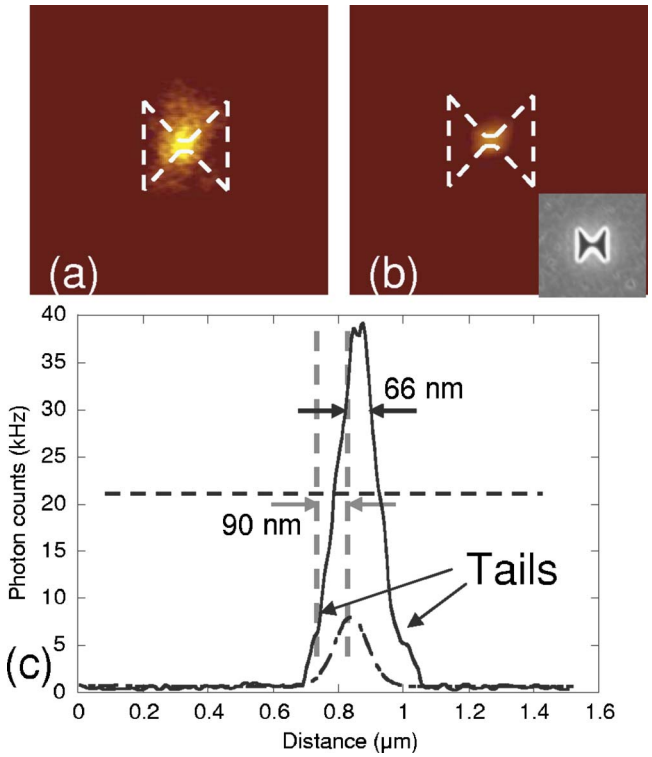

FIG. 3. (Color online) NSOM images obtained by (a) bowtie aperture probe and (b) regular aperture probe. (c) Near-field line profiles of the two NSOM images, and the solid line and dashed line represent bowtie and squarer aperture probes, respectively.

We first characterized the probes by measuring light output from 90×90 nm^2 square apertures in aluminum film (coated on a quartz substrate). The full width at half maximum (FWHM) of the measured light spot is 110 nm, slightly larger than the size of the aperture due to the convolution between the aperture and finite size of the bowtie aperture on the probe. To better characterize the optical resolution of NSOM probes, a smaller or pointlike light source is needed. One can obtain a smaller output light spot from an aperture by reducing its size. However, the optical transmission through subwavelength square aperture decreases drastically as the aperture size is reduced. We have attempted measuring a 40×40 nm^2 square aperture but no signal was detected. On the other hand, a bowtie aperture can also be used to produce a small light spot with much higher transmission efficiency. We characterized bowtie aperture probes by scanning them over bowtie apertures made in aluminum film. For comparison, square aperture probes with an opening of 90×90 nm^2 were also used.

Figures 3(a) and 3(b) show the NSOM images obtained by the bowtie aperture probe and the square aperture probe using the same intensity scale. It was found that the bowtie aperture probe provides near-field measurement counts seven times higher than the regular aperture probe. Line scans of the image shown in Figs. 3(a) and 3(b) are shown in Fig. 3(c). The edge resolutions for both probes measured by 10%–90% criterion of the transmission power are about 90 nm. When using a bowtie aperture probe, a small amount of light can transmit through the arm region of the bowtie aperture. In the NSOM image, two tails were found at the bottom of the scanning profile, as indicated in Fig. 3(c), which were possibly caused by the light leaking through the arm regions of the bowtie aperture. It is also noted from Fig.

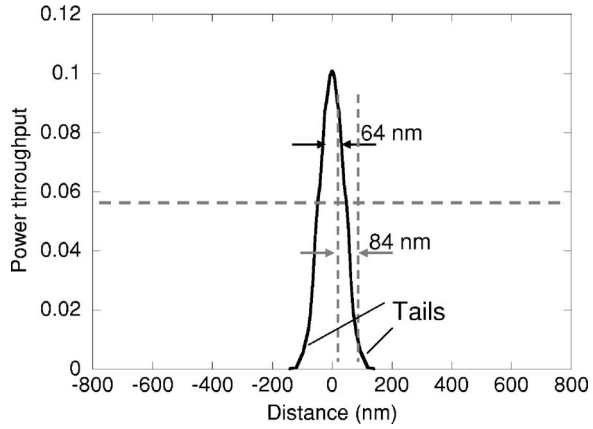

FIG. 4. Scanning profile obtained from the simulation results.

3 that compared with the one obtained using the square aperture probe, the scanning profile obtained using the bowtie aperture probe is different, which has a narrow peak in the middle with a FWHM equal to 66 nm. (A dashed line is drawn across the bottom of the narrow peak.) The FWHM of the peak roughly equals the sum of the two gaps of the two bowtie apertures, which can be explained by the enhanced field in the gap region of the bowtie aperture.

The NSOM images obtained using a bowtie aperture probe were also analyzed using finite difference time domain (FDTD) simulations, which have been previously used to analyze other NSOM imaging processes.[20,21] Commercial software package XFDTD 5.3 from Remcom is used in this work. $4\times4\times4$ nm^3 cells are used to model bowtie nanoapertures. 1400 time steps were run which is determined according to the stability criteria of the FDTD. Debye model parameters of aluminum at 458 nm are found as $\varepsilon_\infty=1$, $\varepsilon_s=-507.825$, $\tau=9.398\times10^{-16}$ s, and $\sigma=4.8\times10^6$ s/m. The simulation geometry includes two 150-nm-thick aluminum layers in contact, with the bottom layer represents the aperture sample. The top layer represents the bowtie probe, consisting of a 180 nm outline bowtie aperture in aluminum followed by a semi-infinite Si_3N_4 layer. Plane wave of wavelength of 458 nm polarized in the direction across the bowtie gap irradiated the sample from the quartz substrate side. In order to simulate the scanning process, the top layer was moved by steps of 8 nm with respect to the bottom layer. Both electric and magnetic components of the transmitted filed were calculated and used to compute the Poynting vectors. Total transmitted power through the bowtie aperture probe was then calculated by integrating the Poynting vectors over the opening cross section of bowtie aperture. Figure 4 plots the power throughput, which is calculated by normalizing the transmitted power to the incident power of the same area. Compared with Fig. 3(c), it can be seen that the calculated near-field image has a similar field distribution with that obtained from NSOM measurement. The calculated edge resolution using the 10%–90% transmission criterion is 84 nm. There is also a narrow peak in the middle of the profile with a FWHM equal to 64 nm. These values match the NSOM results very well.

In summary, we developed NSOM probes with integrated bowtie apertures for enhancing optical transmission in NSOM measurements. Far field measurement results demonstrated that bowtie apertures provided transmitted field intensity one order of magnitude higher than comparable regularly shaped apertures. To characterize the optical resolution of bowtie aperture probes, NSOM measurements using aperture probe were carried out. It was found that the bowtie aperture probe provides high optical transmission compared with a probe with regular shaped aperture. The edge resolution of bowtie aperture probe was larger than the gap size of the bowtie due to the light leaking through the arm. FDTD numerical simulations were carried out and the results matched with experimental findings. This work demonstrated unique properties of bowtie aperture probes compared with regular NSOM probes.

The financial support to this work by the National Science Foundation is acknowledged. Fabrications of aperture samples and NSOM probes by FIB were carried out in the Birck Nanotechnology Center, Purdue University.

[1] D. W. Pohl, W. Denk, and M. Lanz, Appl. Phys. Lett. **44**, 651 (1984).
[2] A. Lewis, M. Isaacson, A. Harootunian, and A. Muray, Ultramicroscopy **13**, 227 (1984).
[3] E. Betzig and R. J. Chichester, Science **262**, 1422 (1993).
[4] I. I. Smolyaninov, D. L. Mazzoni, and C. C. Davis, Appl. Phys. Lett. **67**, 3859 (1995).
[5] E. Betzig, J. K. Trautman, R. Wolfe, E. M. Gyorgy, P. L. Finn, M. H. Kryder, and C. H. Chang, Appl. Phys. Lett. **61**, 142 (1992).
[6] E. H. Synge, Philos. Mag. **6**, 356 (1928).
[7] P. Hoffmann, B. Dutoit, and R. Salathé, Ultramicroscopy **61**, 165 (1995).
[8] D. Zeisel, S. Nettesheim, B. Dutoit, and R. Zenobi, Ultramicroscopy **68**, 2491 (1996).
[9] H. Bethe, Phys. Rev. **66**, 163 (1944).
[10] G. A. Valaskovic, M. Holton, and G. H. Morrison, Appl. Opt. **34**, 1215 (1995).
[11] E. X. Jin and X. Xu, Appl. Phys. Lett. **86**, 111106 (2005).
[12] K. Sendur and W. Challener, J. Microsc. **210**, 279 (2002).
[13] R. Grober, R. Schoelkopf, and D. Prober, Appl. Phys. Lett. **70**, 1354 (1997).
[14] W. Challener, T. Mcdaniel, C. Mihalcea, K. Mountfield, K. Pelhos, and I. Sendur, Jpn. J. Appl. Phys., Part 1 **42**, 981 (2003).
[15] W. Challener, E. Gate, A. Itagi, and C. Peng, Jpn. J. Appl. Phys., Part 1 **45**, 6632 (2006).
[16] L. Wang, S. M. Uppuluri, E. X. Jin, and X. Xu, Nano Lett. **6**, 361 (2006).
[17] E. X. Jin and X. Xu, Appl. Phys. Lett. **88**, 153110 (2006).
[18] J. A. Veerman, A. M. Otter, L. Kuipers, and N. F. Van Hulst, Appl. Phys. Lett. **72**, 3115 (1998).
[19] Y. Mitsuoka, T. Niwa, S. Ichihara, K. Kato, H. Muramatsu, K. Nakajima, M. Shikida, and K. Sato, J. Microsc. **202**, 12 (2001).
[20] O. Martin, J. Microsc. **194**, 235 (1999).
[21] M. Spajer, G. Parent, C. Bainier, and D. Charraut, J. Microsc. **202**, 45 (2001).